REVIEW

Check for updates

Recent advances in metal–organic framework based heterogeneous catalysts for furfural hydrogenation reactions

Qiuju Fu,†[a] Huimin Jiang,†[a] Yujia Wang,[ab] Haiyan Wang*[ab] and Xuebo Zhao ⓘD *[ac]

Metal–organic framework (MOF) based heterogeneous catalysts have been widely used in furfural (FFR) hydrogenation reactions. As numerous studies are related to the conversion of FFR to high value-added chemicals, it is urgently necessary to thoroughly review the recent research progress for better achieving commercial applications in the future. This review summarizes the recent advances, classified by different reaction paths, related to the upgrading of FFR over MOF-based heterogeneous catalysts, including MOFs, MOF derivatives and MOF composites. In addition, some critical issues and perspectives in the hydrogenation of FFR to high-value-added chemicals over MOF-based catalysts are also summarized. This review will provide valuable guidance for the preparation and rational design of MOF-based heterogeneous catalysts for upgrading FFR to high value-added chemicals.

1. Introduction

The rapid economic development and growing demand for non-renewable fossil resources such as coal, oil and natural gas have led to dwindling reserves of fossil energy, promoting researchers seeking environmentally and sustainably alternative energy sources.[1–3] Furfural (FFR), one of the top 30 biomass-derived platform molecules, is mainly obtained by hydrolysis and dehydration of xylose/xylan, which is abundantly available in hemicellulose.[4,5] FFR can be transformed by several catalytic processes, such as hydrogenation, hydrogenolysis, and decarboxylation to a range of high-value-added molecules, which are essential for the production of liquid biofuels, fuel additives and the synthesis of valuable chemicals.[6,7] In the past decades, the production of biofuels and high-value-added chemicals from FFR has received substantial attention.[8–10] There are four primary reaction pathways for the FFR hydrogenation reaction, the products of which are furfuryl alcohol (FFA), tetrahydrofurfuryl alcohol (THFA), 2-methylfuran (2-MF), 2-methyltetrahydrofuran (2-MTHF), cyclopentanone (CPO) and cyclopentanol (CPA), respectively[11] (Fig. 1). The acquisition of

[a] College of Chemistry and Chemical Engineering, China University of Petroleum (East China), Qingdao 266580, China

[b] School of Petrochemical Engineering, Liaoning Petrochemical University, Liaoning 113001, China

[c] School of Materials Science and Engineering, Qilu University of Technology (Shandong Academy of Sciences), Jinan 250353, China

† These authors contributed equally to this work.

Qiuju Fu received her MS degree in 2020 from the China University of Petroleum (East China) under the guidance of Prof. Xuebo Zhao. She is pursuing her PhD degree at the China University of Petroleum (East China) under the guidance of Prof. Xuebo Zhao and Prof. Haiyan Wang. She focuses on the synthesis of metal-based carbon materials derived from MOFs for the hydrogenation of furfural.

Qiuju Fu
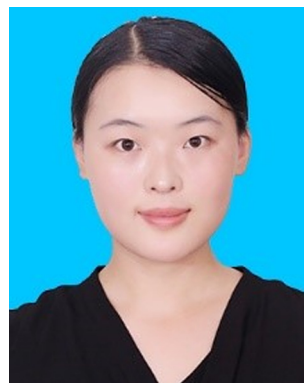
Huimin Jiang received her MS degree from Qingdao University of Science and Technology. She is pursuing her PhD degree at the China University of Petroleum (East China) under the guidance of Prof. Xuebo Zhao and Prof. Jun Zhang. Her research mainly focuses on electrochemical energy storage and conversion materials derived from MOFs.
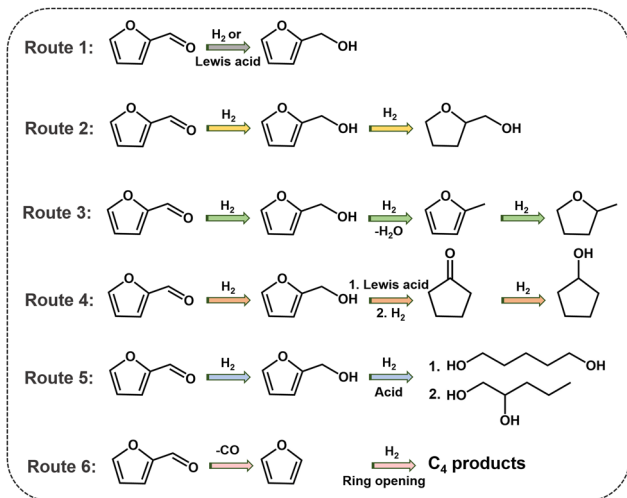
Huimin Jiang

Fig. 1 Routes for the hydrogenation of FFR into high value-added chemicals.

demands high hydrogenation activity of metals for catalysis. 2-MF and 2-MTHF are generated by the initial hydrogenation of FFR to afford FFA, followed by the hydrogenolysis of the C–O bonds, which requires a catalyst for achieving consecutive hydrodeoxygenation catalytic processes. For obtaining CPO or CPA, a complicated sequence of steps is needed, including the hydrogenation of C=O, ring rearrangement, hydrogenation, and dehydration, which necessitates a metal–acid bifunctional catalyst. In addition, FFR can be converted to highly valuable furans such as 1,2-pentanediol, 1,5-pentanediol and a range of C_4 products through other routes, such as decarbonization, ring opening and hydrolysis. Since both the furan ring and the aldehyde group contained in the FFR molecule are highly active, the selective hydrogenation of FFR to target products is challenging. Many strategies, such as impregnation,[12] alloying,[13] in situ conversion,[14] co-assembly,[15] and multiple active species,[16] have been reported for designing catalysts towards the hydrogenation of FFR. It is worth mentioning that many pioneering advances have been achieved in the hydrogenation of FFR through rational designing and optimizing catalysts.

Metal–organic frameworks (MOFs) are a class of crystalline porous materials assembled by metal ions/clusters and multidentate organic ligands, which possess many merits, such as large surface area, adjustable pore sizes, and easy functionalization.[17–19] The outstanding adjustable features and large homogeneous pores of MOFs offer considerable promise for heterogeneous catalytic applications.[20,21] Although MOF materials have shown excellent catalytic performance in specific fields, the activity in the majority of fields remains unsatisfactory. Therefore, many endeavors have been devoted to designing efficient catalysts for applications in various fields.[22,23] One is to modify the metal nodes or organic ligands in the framework of MOFs to expose more active sites, which applies to reactions catalyzed by metal nodes in MOFs.[24,25] Owing to the tunable pore size and surface area, MOFs can be used as precursors to incorporate guest species, such as the in situ introduction or impregnation, for fabricating MOF-based composites with desired compositions.[26,27] As porous materials, the pore channels of MOFs provide a good opportunity for confining the guest particles, preventing agglomeration of nanoparticles and

FFA is merely the hydrogenation of the aldehyde group, which is generally catalyzed by metals with moderate hydrogenation activity or metals with a Lewis acid site for transfer hydrogenation. Unlike FFA, the synthesis of THFA requires successive hydrogenation of the aldehyde group as well as the furan ring, which

Yujia Wang received her MS degree from Liaoning Petrochemical University. She is pursuing her PhD degree at the China University of Petroleum (East China) under the guidance of Prof. Zhanxu Yang and Prof. Haiyan Wang. She focuses on the synthesis of platinum single-atoms on S-vacancy rich MoS_{2-x} for the hydrogenation of furfural and its derivatives.

Yujia Wang

Prof. Haiyan Wang received his PhD degree in 2002 from Harbin Institute of Technology. His scientific interests are focused on the development of novel catalytic materials and catalysts for industrial catalysts, such as the modification of zeolites and the preparation of transition metal phosphides and carbides and their energy applications.

Haiyan Wang

Prof. Xuebo Zhao received his PhD degree in 2005 from Newcastle University. His scientific interests are focused on the development of advanced materials for sustainable energy storage, such as the synthesis of new carbon materials, metal–organic frameworks, and their energy applications.

Xuebo Zhao

maximizing the surface area of the guest molecules exposed. Most importantly, the periodic arrangement of inorganic and organic components in MOFs enables the transformation into metal nanoparticles and carbonaceous materials as self-sacrificing templates.[28–30] These MOF derivatives, possessing highly dispersed targeted active sites, excellent stability, controllable heteroatomic doping and large surface areas, hold tremendous promise in catalytic applications.[31] In conclusion, MOF-based catalysts, which are convenient to prepare, reproducible, with well-preserved morphology and homogeneous exposure of active sites, show promising potential as heterogeneous catalysts for FFR hydrogenation.

Although encouraging summaries of the conversion of FFR to high-value-added chemicals are available, MOF-based catalysts lack detailed presentation and summarization.[5,32–34] Herein, recent applications of MOF-based heterogeneous catalysts for the hydrogenation of FFR are summarized from the perspectives of the preparation FFA, THFA, 2-MF/2-MTHF and CPO/CPA (Fig. 2). At present, MOF-based catalysts can be classified as MOFs, MOF composites and MOF derivatives. This review aims to summarize the preparation of MOF-based catalysts for FFR hydrogenation reactions and to compare the active species of different reaction routes, facilitating the engineering of catalysts for efficient conversion of FFR to target products in the future.

2. Catalytic hydrogenation of furfural to furfuryl alcohol

Furfuryl alcohol (FFA), the most important chemical derived from FFR, is widely used in the polymer industry for furan resins, furfural resins and phenolic resins, as well as fine chemical industries for pharmaceutical intermediates, lubricants, adhesives and dispersants.[35] The hydrogenation reaction of FFA from FFR occurs on the carbonyl group outside the furan ring. Satisfactory achievements, such as high activity and selectivity, have been made using both noble and non-noble catalysts (Table 1). The development of an MOF encapsulated metal catalyst is regarded as an effective way to modulate the catalytic selectivity owing to the unique channels of the MOF.[36,37] UiO-66, with excellent thermal and chemical stability, is the most frequently reported material for loading noble metals, which performs better in the hydrogenation of FFR to FFA.[38–40] Long and co-workers constructed a Pt/CeO$_2$@MOF core@shell hybrid sample *via* a sodium polystyrenesulfonate (PSS)-induced and microwave-assisted route (Fig. 3a).[41] PPS altered the surface charge of Pt/CeO$_2$ to speed the adsorption of metal ions, and microwave heating facilitated the oriented nucleation and growth of MOF shells on the Pt/CeO$_2$ nanospheres. The thickness of the MOF shells can be easily tuned by controlling the MOF synthesis. The obtained Pt–CeO$_2$@UiO-66-NH$_2$ sample exhibited remarkable catalytic performance with high FFR conversion (99.3%) and FFA selectivity (>99%) for selective hydrogenation of FFR to FFA. Subsequently, Zhang's group encapsulated bimetallic catalysts in MOF
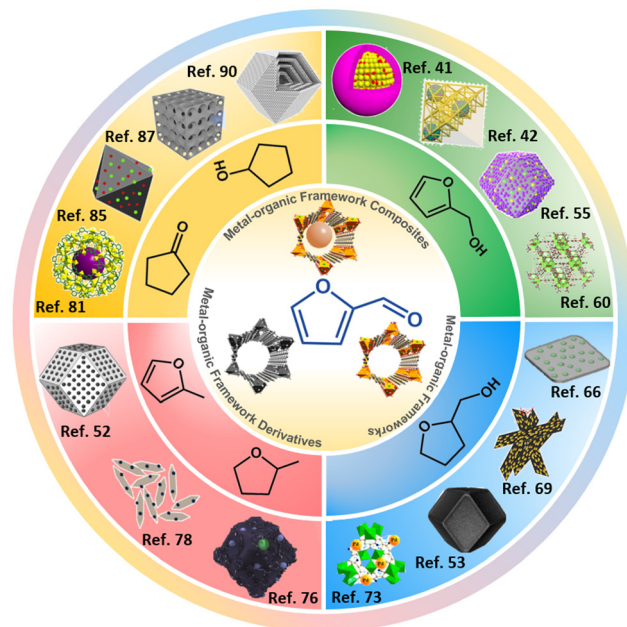

Fig. 2 Metal–organic framework-based heterogeneous materials for the synthesis of high value-added chemicals in furfural hydrogenation reactions. Reproduced with permission from ref. 41, copyright (2018) American Chemical Society. Reproduced with permission from ref. 42, copyright (2020) American Chemical Society. Reproduced with permission from ref. 55, copyright (2021) American Chemical Society. Reproduced with permission from ref. 60, copyright (2022) Elsevier. Reproduced with permission from ref. 66, copyright (2017) Royal Society of Chemistry. Reproduced with permission from ref. 69, copyright (2020) Elsevier. Reproduced with permission from ref. 53, copyright (2021) Elsevier. Reproduced with permission from ref. 73, copyright (2018) Elsevier. Reproduced with permission from ref. 76, copyright (2022) Elsevier. Reproduced with permission from ref. 78, copyright (2020) American Chemical Society. Reproduced with permission from ref. 52, copyright (2020) Elsevier. Reproduced with permission from ref. 81, copyright (2019) Elsevier. Reproduced with permission from ref. 85, copyright (2016) Elsevier. Reproduced with permission from ref. 87, copyright (2021) Wiley-VCH. Reproduced with permission from ref. 90, copyright (2019) American Chemical Society.

frameworks to investigate the effect of MOF frameworks on the electronic and geometrical structure of metals.[42] A series of Pt–Sn nanoparticles with different Sn/Pt ratios were encapsulated in UiO-66-NH$_2$ (Pt–Sn@UiO-66-NH$_2$) by an impregnation–reduction strategy. Compared to Pt@UiO-66-NH$_2$, the PtSn$_{0.1}$@UiO-66-NH$_2$ sample, with only 10% Sn added, showed significantly improved activity and stability during the hydrogenation of FFR to FFA, which is attributed to the multiple synergistic effects of Pt, Sn and –NH$_2$ groups in the MOF framework. In addition to UiO-66, Zr-BTC has been reported as promising support for encapsulating noble metals, which showed excellent performance in the catalytic hydrogenation of FFR.[43] Zahid *et al.* designed a series of catalysts loaded with Pt–Co intermetallic nanoparticles (IMNs) on MIL-101(Cr) *via* a polyol method.[44] There exist electronic and geometric effects during the charge transfer between Co and Pt, which enhance the catalytic activity and selectivity. Notably, the 3%Pt3%Co/MIL-101(Cr) catalyst achieves 97% FFR conversion and 94% FFA selectivity under mild conditions.

630 | *Mater. Chem. Front.*, 2023, **7**, 628–642

This journal is © The Royal Society of Chemistry and the Chinese Chemical Society 2023

Table 1 The conversion of FFR to FFA over MOF-based catalysts

MOF	Catalyst	Solvent	H_2(MPa)	Temp. (°C)	Time (h)	FFR Conv. (%)	FFA Yield (%)	Ref.
UiO-66	UiO-66-Pd-0.96%	2-propanol	2	110	4	71	66.7	38
UiO-66	Ru/UiO-66	H_2O	0.5	20	4	–	94.9	39
UiO-66	Pd/H-UiO-66	H_2O	0.5	60	3	100	99	40
UiO-66-NH_2	Pt–CeO_2@UiO-66-NH_2	2-propanol	1	80	54	99.3	98.3	41
Zr-BTC	Ru/Zr-BTC	H_2O	0.2	20	4	100	99.4	43
Zr-BTC	Pd/Zr-BTC	H_2O	0.2	20	4	100	98.4	43
MIL-101(Cr)	3%Pt3%Co/MIL-101(Cr)	2-propanol	1	60	2	97	91.2	44
HKUST-1	HK-1-350	ethanol	1.5	120	3	100	100	45
HKUST-1	CuO#SiO_2−s1	ethanol	2.5	140	2	100	100	46
ZJU-35	ZJU-35-400	2-propanol	1	130	3	38.5	26.4	47
ZJU-36	ZJU-36-350	2-propanol	1	130	3	82.4	78.2	47
ZJU-199	ZJU-199-350	2-propanol	1	130	3	97.1	97	47
Cu-BTC	CuCo$_{0.4}$/C-873	ethanol	3	140	1	98.7	96.4	48
CoNi-MOF	2Co-1Ni@NC-800	methanol	2	120	1	100	99	49
MIL-96	Ni$_{0.15}$/Al$_2$O$_3$-C	ethanol	4	160	6	98.7	92	50
ZIF-67	Co-900	H_2O	2	60	5	100	100	51
ZIF-67	10-Cu/ZIF	2-propanol	2	180	5	73.9	44.6	52
ZnCo-ZIF	ZnCo-US@NC-700	ethanol	2	120	4	100	91.5	53
CuCoZn-ZIF	CuCo/Zn@NPC-600	tetrahydrofuran	2	140	4	99.9	99.9	54
NiCoZn-ZIF	NiCoZn@CN-600	tetrahydrofuran	2	160	4	100	99	55
ZIF-8	MoC/NCNCs	2-propanol	3	135	–	99.5	97.8	57
CuCoZn-ZIF	CuCo/Zn@NPC-600	2-propanol	–	130	7	95.8	94.9	54
MOF-808	M-MOF-808	2-propanol	–	100	2	99.2	93	58
MOF-808	D$_{40}$-MOF-808	2-propanol	–	90	2	99	93.5	59
UiO-66	UiO-S$_{0.6}$	2-propanol	–	150	6	98.7	94.7	60
UiO-66	UiO-66	2-propanol	–	140	5	99	97	61
DUT-52	DUT-52	2-propanol	–	160	3	99	99	62

Cu-MOFs are ideal templates for the fabrication of porous Cu-based catalysts for the hydrogenation of FFR to FFA. Du et al. synthesized a series of carbon-supported Cu-based catalysts (HK-1-T) via one-step pyrolysis conversion of HKUST-1[45] (Fig. 3b). HK-1-350 featured excellent reusability, with 100% FFR conversion and FFA selectivity obtained within 2 h at 120 °C and 1.5 MPa H_2. Yang et al. fabricated a mesoporous silica-supported Cu-based (CuO#SiO_2) catalyst by pyrolyzing H-KUST-1#SiO_2 composites.[46] The metal dispersion and reducibility during calcination could be tuned by introducing silica. Excellent activity was achieved on the optimized CuO#SiO_2-s1, with nearly 100% yield toward FFA. Chen et al. prepared a ZJU-199-350 catalyst with Cu/Cu_2O nanojunctions encapsulated and stabilized in porous organic frameworks by modulating the acrylate contents in ZJU-199 and the pyrolysis conditions[47] (Fig. 3c). The acrylate groups not only enhance the polymerization degree of MOFs, but also play an essential role in the generation and stabilization of highly dispersed and accessible Cu/Cu_2O heterojunctions. The ZJU-199-350 sample with abundant Cu/Cu_2O sites exhibited excellent catalytic properties in converting FFR to FFA, obtaining 97% yield of FFA.

Bimetallic catalysts are extensively used in the conversion process from FFR to FFA. Wang et al. fabricated a CuCo bimetallic catalyst derived from Co-doped Cu-BTC for the hydrogenation of FFR.[48] The introduction of Co contributes to the dispersion of Cu and Co particles, while the thermal decomposition temperature affects both the size and chemical state of the particles. The best catalytic performance is achieved on CuCo$_{0.4}$/C-873, giving 98.7% FFR conversion and 97.7% FFA selectivity. Huang et al. reported a series of highly dispersed Co–Ni alloy particles encapsulated in porous N-containing

carbon support catalysts (xCo–yNi@NC) by pyrolyzing the CoNi-MOF for the conversion of FFR[49] (Fig. 3d). Co–Ni alloys exhibited a strong synergistic effect, and the presence of N species modulated the physicochemical properties of the catalyst, which enhances the catalytic performance. In addition, the solvent played a vital role in product distribution. Among them, the 2Co–1Ni@NC-800 catalyst achieved 99% FFA yield in methanol at 120 °C and 2 MPa H_2 for 1 h. Ni-based catalysts are also used for FFR to FFA conversions. Hu et al. constructed a Ni/Al_2O_3-C catalyst by using Ni-loaded MIL-96 as the precursor.[50] Benefiting from the Al_2O_3-C support, Ni particles are uniformly dispersed in the hexagonal platelet matrix. 98.7% FFR conversion and 92% FFA selectivity were achieved over Ni$_{0.15}$/Al$_2$O$_3$-C.

ZIF-67, the most commonly used Co-based MOFs, was often used as the precursor to synthesize mono-, bi- and tri-metallic catalysts for the hydrogenation of FFR to FFA. Gong et al. exploited ZIF-67-derived N-doped carbon nanotubes for confining Co particles with Co–N_x active sites, which exhibited remarkable catalytic activity and stability for biomass-derived unsaturated compounds.[51] The Co–N_x sites in Co-900 play a crucial role in the selective hydrogenation performance, giving 100% FFA yield within 5 h at 60 °C and 2 MPa H_2 using water as the solvent. The influence of introducing Cu on the selectivity of FFR hydrogenation was investigated by Lee et al. through incorporating Cu into ZIF-67.[52] The selectivity can be altered from 2-MF to FFA after introducing the Cu species. A series of N-doped carbon-coated bimetallic composites (ZnCo-ZIF-US-T) were synthesized from ZnCo-ZIF.[53] The prepared ZnCo-US@NC-700 catalyst showed excellent catalytic performance from FFR to FFA. Fan et al. designed a series of Cu, Co, Zn
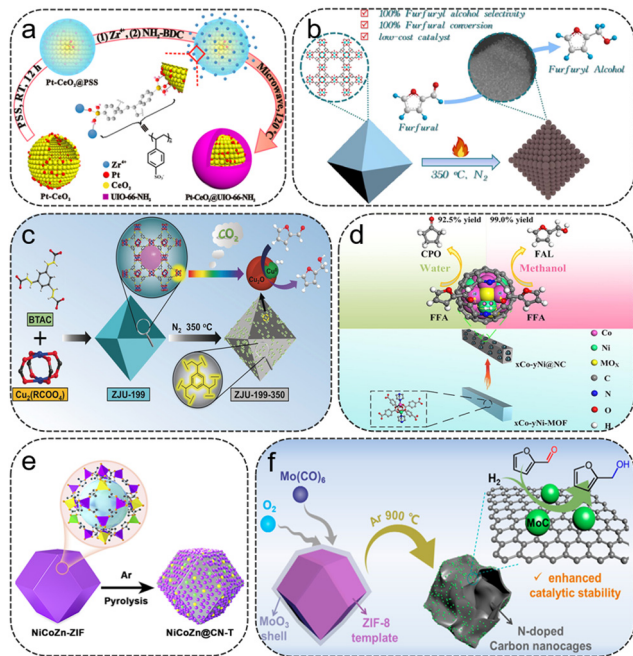
This journal is © The Royal Society of Chemistry and the Chinese Chemical Society 2023

Mater. Chem. Front., 2023, 7, 628–642 | 631

Fig. 3 (a) Schematic illustration for the formation of PtCeO$_2$@UiO-66-NH$_2$. Reproduced from ref. 41 with permission from American Chemical Society, copyright 2018. (b) Schematic illustration of the preparation of HK-1-350 catalysts for hydrogenation of FFR into FFA. Reproduced from ref. 45 with permission from Elsevier, copyright 2022. (c) Schematic illustration of the preparation of Cu/CuO$_x$ nanoparticles for liquid phase hydrogenation of FFR into FFA. Reproduced from ref. 47 with permission from Wiley-VCH, copyright 2019. (d) Schematic illustration of the preparation of xCo−yNi@NC catalysts for the hydrogenation of FFR into FFA. Reproduced from ref. 49 with permission from Wiley-VCH, copyright 2019. (e) Schematic illustration of the synthesis of NiCoZn@CN-T. Reproduced from ref. 55 with permission from American Chemical Society, copyright 2021. (f) Schematic illustration of the preparation of MoC/NCNCs catalyst for FFR to FFA. Reproduced from ref. 57 with permission from American Chemical Society, copyright 2022.

modified N-doped porous carbon (CuCo/Zn@NPC) samples using polymetallic CuCoZn-ZIF as the precursor for the hydrogenation of FFR to FFA.[54] The CuCo/Zn@NPC-600 catalyst exhibited remarkable catalytic activity with almost complete FFR conversion and 100% FFA selectivity at 140 °C and 2 MPa H$_2$ for 4 h. In addition, the CuCo/Zn@NPC-600 catalyst gave 94.9% FFA yield at 130 °C for 7 h when using 2-propanol as the hydrogen donor. The remarkable performance of CuCo/Zn@NPC-600 is correlated with the highly dispersed metal particles, and the unique porous structure was retained after the escape of Zn, and the synergistic effect provided by Cu and Co. Subsequently, Li et al. synthesized a multimetallic catalyst (NiCoZn@CN) derived from the multimetal doped NiCoZn-ZIF,[55] obtaining 99% FFA yield at 160 °C for 4 h (Fig. 3e). In the NiCoZn@CN sample, Co^0 is the main active site, the contents of which are related to Ni and Zn doping. The doping of Ni benefits the activation of H$_2$, while the doping of Zn facilitates the dispersion of metal particles. The application of molybdenum carbides for FFR hydrogenation was also investigated and they showed superior selectivity for FFA.[56,57] Wang et al. successfully constructed functionalized N-doped carbon

nanocages (NCNCs) for FFR hydrogenation via a one-stone-two-birds strategy[57] (Fig. 3f). The existence of Mo(CO)$_6$ prevented the collapse of the ZIF-8 precursor in the thermal treatment process and converted it into MoC active sites anchored to the NCNCs after pyrolysis. This one-stone-two-birds strategy has been verified to be adaptable to prepare Cr- and W-decorated NCNCs. High FFR conversion (99.5%) and FFA selectivity (97.8%) could be achieved by using MoC/NCNCs as the catalyst in 2-propanol at 135 °C and 3 MPa H$_2$.

Recently, catalytic transfer hydrogenation (CTH), in which high-pressure H$_2$ is substituted by hydrogen donors (e.g. secondary alcohols), has attracted considerable attention and has been proven to be highly selective for conversion from FFR to FFA.[9] Therefore, recent advances using MOF as the precursor in the CTH from FFR to FFA are briefly discussed and summarized in Table 1. Zr-based MOFs, which possess an abundance of active metal nodes, are widely used in CTH reactions.[63] H. Valekar et al. synthesized an M-MOF-808 sample via a simple methanol activation process, exhibiting excellent performance in the CTH reaction of FFR even at room temperature.[58] The activation process altered the acid–base properties of the MOF-808 surface due to the increase of coordinatively unsaturated sites, hydroxyl and methoxy groups in MOF-808, facilitating the adsorption of FFR and 2-propanol molecules. In addition, a reaction mechanism for the CTH reaction of FFR on M-MOF-808 was proposed in detail using isotopically labelled 2-propanol-d$_8$ experiments and DFT calculations (Fig. 4a). Our previous work synthesized a series of defective MOF-808 (D$_x$-MOF-808) samples by modification with benzoic acid (HBC) (Fig. 4b).[59] HBC was introduced as a temporary ligand and as a terminating agent to modulate the particle size. The degree of ligand deficiency and the number of exposed Zr sites can be well-regulated by varying the amount of HBC. Excellent performance of 99% FFR conversion and 94.4% FFA selectivity was reached over the D$_{40}$-MOF-808 sample within 2 h at 90 °C with 2-propanol as the hydrogen donor. It was shown that the catalytic activity of the catalysts is highly correlated with the number of exposed Zr sites, the degree of missing linkers and the surface area. Additionally, the D$_{40}$-MOF-808 sample had robust stability without significant loss of catalytic activity after five cycles, and was adapted to the hydrogenation of a range of biomass-derived compounds. In addition to MOF-808, UiO-66 has also been used for the CTH reaction from FFR to FFA, all achieving remarkable catalytic performance.[60,61] Wu and the co-workers reported a series of UiO-66 functionalized by sulfonic groups (UiO-S$_x$), which exhibit high FFA selectivity in the CTH reaction (Fig. 4c).[60] The modification of sulfonic groups on UiO-66 was demonstrated to form more strongly Lewis acidic–basic and Brønsted acidic sites, and a remarkable catalytic activity of 94.7% FFA yield was obtained at 150 °C for 6 h over the UiO-S$_{0.6}$ catalyst with 2-propanol as the hydrogen donor. Isotope labelling experiments showed that the β-H in 2-propanol transferred to the α-C of FFR via the six-membered transition state at the Lewis acidic–basic and Brønsted acidic sites of UiO-S$_{0.6}$, which is the rate-determining step in the formation of FFA. Qiu et al. prepared isoreticular

632 | *Mater. Chem. Front.*, 2023, **7**, 628–642

This journal is © The Royal Society of Chemistry and the Chinese Chemical Society 2023
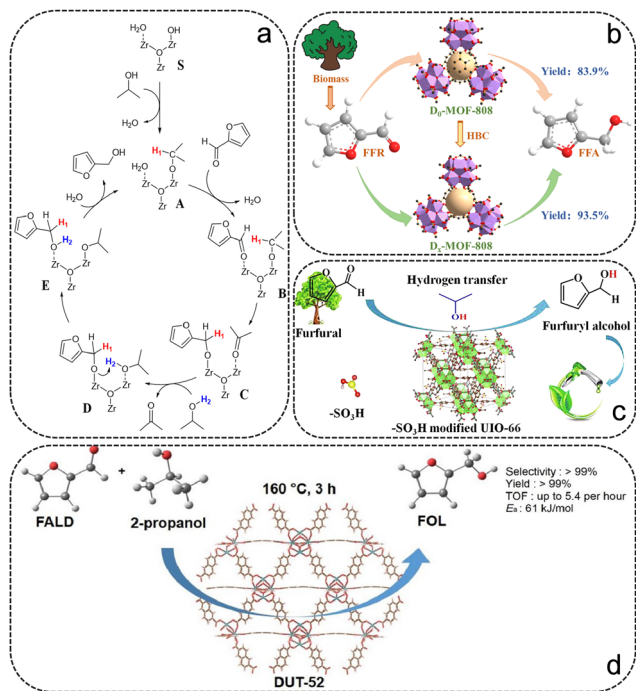
Fig. 4 (a) The proposed CTH reaction path. Reproduced from ref. 58 with permission from American Chemical Society, copyright 2020. (b) Schematic illustration of the preparation of D_{40}-MOF-808 catalysts for CTH of FFR. Reproduced from ref. 59 with permission from Elsevier, copyright 2022. (c) Schematic illustration of the preparation of $-SO_3$ modified UiO-66 for CTH of FFR. Reproduced from ref. 60 with permission from Elsevier, copyright 2022. (d) Schematic illustration of CTH reaction of FFR over DUT-52. Reproduced from ref. 62 with permission from Elsevier, copyright 2022.

DUT-52 with higher Lewis acidity to convert FFR to FFA (Fig. 4d).[62] The DUT-52 catalyst exhibited good stability, with more than 99% FFA yield at 160 °C for 3 h under 2-propanol.

3. Catalytic hydrogenation of furfural to tetrahydrofurfuryl alcohol

Tetrahydrofurfuryl alcohol (THFA), a biodegradable and environmentally benign furanic chemical extensively used in many agricultural and industrial applications, is a promising intermediate to prepare diols. The conversion of THFA from FFR involves the hydrogenation of both the carbonyl group and the furan ring, via FFA as the intermediate. It is reported that Ni-based catalysts offer the advantages of low price and high hydrogen activation capacity and the ability to promote parallel adsorption of FFR molecules, resulting in high activity and selectivity for THFA.[64] Therefore, Ni-MOFs were the optimal choice for preparing catalysts. Only a few studies have reported the use of MOF-derived catalysts for FFR to THFA conversions, as listed in Table 2.

Guo's group fabricated a series of Ni-based catalysts (Ni-MFC-X) through pyrolyzing the 2D Ni-MOF, which displayed promising performance in the hydrogenation reaction of FFR.[65] Su and co-workers reported a carbon-embedded Ni/C catalyst synthesized by employing Ni-BTC as the sacrificial template, which exhibits excellent catalytic performance for the conversion of FFR to THFA due to the Ni particles uniformly embedded in the ligand-derived carbon (Fig. 5a).[66] The catalytic performance of the as-prepared Ni/C catalysts is greatly influenced by the heat treatment conditions, the composition of the Ni-BTC precursor and the catalytic conditions. The Ni/C-500 sample displayed the best catalytic activity with 100% THFA yield at 120 °C and 1 MPa H_2 for 2 h, which is highly related to the uniformly dispersed Ni particles (14 nm) and its highest BET surface area. Subsequently, they constructed Ni particles implanted in carbon matrix (Ni/C) aerogels through water-induced self-assembly of Ni-BTC, followed by pyrolysis carbonization.[67] The Ni/C_{500} aerogels showed high catalytic activity toward the hydrogenation of FFR to THFA in the aqueous phase. To improve the catalytic performance, many endeavors have been attempted. Wang et al. constructed a Ni@C@CNT composite by pyrolyzing Ni-MOF doped with carbon nanotubes (CNTs).[68] The introduction of CNTs promoted the formation of Ni_3C species and reduced the metal particle size, which plays a vital role in achieving good performance of the Ni@C@CNT catalyst. Tang et al. reported an alloy chemistry strategy to modulate the d-band center of Ni by introducing Cu for the selective hydrogenation of FFR.[69] A series of Ni–Cu alloy samples were prepared by employing

Table 2 The conversion of FFR to THFA over MOF based catalysts

MOF	Catalyst	Solvent	H_2 (MPa)	Temp. (°C)	Time (h)	FFR Conv. (%)	THFA Yield (%)	Ref.
Ni-(tia)($H_2O)_2]_n$	Ni-MFC-700	methanol	2	160	4	91.8	46.8	65
Ni-BTC	NiC/500	2-propanol	1	120	2	100	100	66
Ni-BTC	Ni/C_{500} aerogel	H_2O	4	160	5	93.9	6.9	67
Ni-BTC	Ni@C@CNT	ethanol	4	120	4	99.1	94.7	68
NiCu-BTC	$NiCu_2$/C	ethanol	3	150	3	98.7	38.6	69
NiCu-BTC	NiCu/C	ethanol	3	150	3	99.9	64.1	69
NiCu-BTC	$NiCu_{0.25}$/C	ethanol	3	150	3	99.9	94.8	69
NiCu-BTC	$NiCu_{0.33}$/C	ethanol	3	150	3	99.9	94.6	69
NiCo-BTC	Ni_3Co_1@C	H_2O	1	80	1	99	95	70
ZIF-67	Co@NC-700	ethanol	2	120	4	100	90	53
UiO-66	Pd/UiO-66	H_2O	1	60	4	100	100	72
MIL-101(Cr)-NH_2	Pd@MIL-101(Cr)-NH_2	H_2O	2	40	6	99.9	99.6	73
ZIF-67	$PdCo_3O_4$@NC	2-propanol	2.5	150	6	100	95	74
ZIF-67	$PdFeo_3O_4$@NC	2-propanol	2	150	8	100	70	74

This journal is © The Royal Society of Chemistry and the Chinese Chemical Society 2023

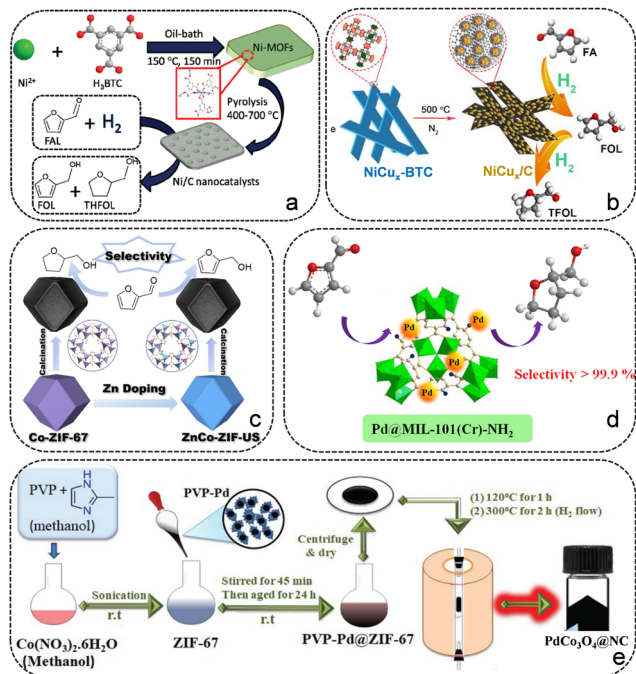Mater. Chem. Front., 2023, 7, 628–642 | 633

Fig. 5 (a) Synthesis of Ni/C catalysts for the hydrogenation of FFR to THFA. Reproduced from ref. 66 with permission from Royal Society of Chemistry, copyright 2017. (b) Schematic illustration of the synthesis procedure for catalyst NiCu$_x$/C. Reproduced from ref. 69 with permission from Elsevier, copyright 2020. (c) Synthesis of Co@NC catalysts for the selective hydrogenation of FFR. Reproduced from ref. 53 with permission from Elsevier, copyright 2021. (d) Schematic illustration of Pd@MIL-101(Cr)-NH$_2$ for the conversion of FFR to THFA. Reproduced from ref. 73 with permission from Elsevier, copyright 2018. (e) Schematic illustration of the MOF-mediated synthesis of PdCo$_3$O$_4$ nanoparticles on N-doped porous carbon sheets. Reproduced from ref. 74 with permission from Royal Society of Chemistry, copyright 2019.

NiCu$_x$-BTC as the self-sacrificing template (Fig. 5b). DFT calculations showed that Ni exhibits a downshift d-band center after alloying with Cu, which can facilitate the desorption of dissociated H species from Ni to enhance the catalytic activity and change the adsorption orientation of FFR to modulate the product distribution. NiCu$_{0.33}$/C and NiCu$_{0.25}$/C catalysts both gave almost complete FFR conversion and more than 94.5% THFA yield at 150 °C and 3 MPa H$_2$ for 3 h in ethanol. Xia *et al.* synthesized an array of NiCo bimetallic catalysts with uniformly dispersed metal particles on porous carbon for the hydrogenation of FFR.[70] The Ni$_3$Co$_1$@C catalyst achieved 95% THFA yield at 80 °C and 1 MPa for 1 h under aqueous medium. The addition of Co to the bimetallic catalysts reduced the particle size, which improved the dispersion of metal particles and the catalytic activity. Additionally, the ZIF-67-derived Co@NC-700 catalyst was prepared *via* a simple one-step pyrolysis strategy, giving 90% yield of THFA at 120 °C and 2 MPa H$_2$ for 4 h (Fig. 5c).[53]

The introduction of noble metals into the MOF framework to further generate noble metal/MOF or noble/transition metal composites has been reported to facilitate the conversion of FFR to THFA. Noble metal/MOF compounds have been shown

to achieve high catalytic performance in FFR hydrogenation.[71] Wang *et al.* synthesized a Pd/UiO-66 catalyst with well-dispersed Pd particles for the hydrogenation of FFR to THFA, obtaining a 100% yield of THFA under mild conditions.[72] With the strong adsorption capacity between FFR and UiO-66, Pd/UiO-66 exhibited higher activity than Pd/SiO$_2$ and Pd/γ-Al$_2$O$_3$. Yin *et al.* prepared an efficient Pd@MIL-101(Cr)-NH$_2$ catalyst for the conversion of FFR to THFA by an anionic exchange followed by H$_2$ reduction methods (Fig. 5d).[73] The existence of –NH$_2$ in MOFs facilitates the dispersion of Pd particles and improves the interactions between the intermediate FFA and the support, which is beneficial for further hydrogenation of FFA to THFA. A complete FFR conversion was achieved on Pd@MIL-101(Cr)-NH$_2$ with 99.6% selectivity of THFA at 40 °C for 6 h. Precious-transition metal composites have been reported to be an alternative way to obtain effective catalysts used for the upgrading and conversion of biomass-derived FFR. Pendem *et al.* reported the preparation of PdCo$_3$O$_4$ or PdFe$_3$O$_4$ particles encapsulated in N-doped carbon catalysts by pyrolyzing a Pd-modified MOF (Fig. 5e).[74] The as-prepared PdCo$_3$O$_4$/NC catalyst afforded a 95% THFA yield after a 6 h reaction at 150 °C and 2.5 MPa H$_2$, but the PdFe$_3$O$_4$/NC catalyst only afforded a THFA yield of 70% even at 8 h. The superior catalytic activity and stability are attributed to the presence of PdCo-N$_x$ active sites, the synergistic effects between Co$_3$O$_4$ and Pd, and the existence of N species in the carbonaceous matrix.

4. Catalytic hydrogenation of furfural to 2-methyl furan and 2-methyl tetrahydrofuran

As typical products, 2-methyl furan (2-MF) and 2-methyl tetrahydrofuran (2-MTHF) can be applied directly as bioethanol substitutes in gasoline and as synthetic diesel additives, and have aroused attractive interest due to their appealing properties.[75] Generally speaking, 2-MF was acquired by selective hydrogenation of FFR to obtain FFA, followed by hydrogenolysis of the C–O bonds. At present, there are comparatively few reports on MOF-based catalysts catalyzing FFR to 2-MF/2-MTHF, as shown in Table 3. Gyeong Lee *et al.* reported a series of ZIF-67-derived Co-based catalysts obtained at different temperatures and pyrolysis times, which were equipped with metallic Co particles on N-doped carbon (Co/NC) (Fig. 6a).[52] The most active Co/NC catalyst, with a well-retained morphology of the ZIF-67 precursor and uniformly distributed Co particles supported on N-doped carbon, was obtained at 400 °C under a H$_2$/Ar atmosphere. The improved catalytic activity and 2-MF selectivity were obtained on the Co/NC-400 catalyst with longer reduction times, which possessed more contents of Co^0. The Co/NC-400-6 catalyst exhibited the highest FFR activity, giving 100% FFR conversion and 57.5% 2-MF selectivity at 180 °C and under 2 MPa H$_2$ for 10 h. The doping of the second metal has a significant effect on the electronic structure of the active site and the catalytic performance. Huang *et al.* synthesized a series of Zn-doped Co/NC catalysts

634 | *Mater. Chem. Front.*, 2023, **7**, 628–642

This journal is © The Royal Society of Chemistry and the Chinese Chemical Society 2023

Table 3 The conversion of FFR to 2-MF and 2-MTHF over MOF based catalysts

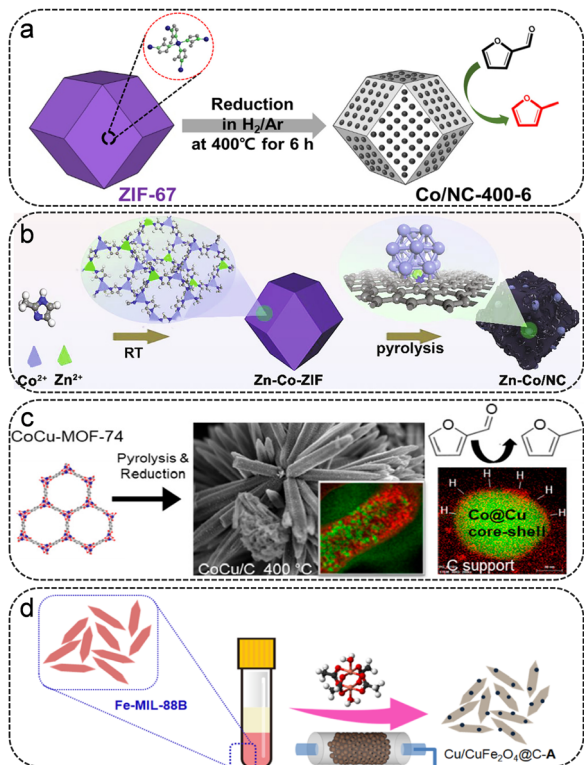| MOF	Catalyst	Solvent	H$_2$ (MPa)	Temp. (°C)	Time (h)	FFR Conv. (%)	2-MF Yield (%)	2-MTHF yield	Ref.
ZIF-67	Co/NC-400-2	2-propanol	2	180	10	100	54.7	–	52
ZIF-67	Co/NC-400-6	2-propanol	2	180	10	100	57.5	–	52
ZnCo-ZIF	Zn-Co/NC-1	2-propanol	1	200	8	100	0.1	93.8	76
Fe-MIL-88B	Cu/CuFe$_2$O$_4$@C-A	2-propanol	1.5	165	5	100	100	–	78

Fig. 6 (a) Synthesis of Co/NC-400-6 catalysts from ZIF-67. Reproduced from ref. 52 with permission from Elsevier, copyright 2020. (b) Schematic illustration of the synthesis of Zn–Co/NC for the conversion of FFR to 2-MTHF. Reproduced from ref. 76 with permission from Elsevier, copyright 2022. (c) Schematic illustration of the synthesis of CoCu/C particles for FFR to 2-MF. Reproduced from ref. 77 with permission from Elsevier, copyright 2019. (d) Synthesis of Cu/CuFe$_2$O$_4$@C-A catalysts from Fe-MIL-88. Reproduced from ref. 78 with permission from American Chemical Society, copyright 2020.

by employing bimetallic Zn–Co-ZIF as the self-sacrificial template for the conversion of FFR to 2-MTHF (Fig. 6b).[76] The Zn–Co/NC-1 catalyst, which possessed a trace amount of Zn dopant (0.38%), showed the best catalytic performance, with a 93.8% yield of 2-MTHF at 200 °C for 8 h. The Zn atoms are not only doped in the carbon support but also partially incorporated into the Co particles. The theoretical calculations verified that the doping of Zn facilitates the electron transfer from the carbon support to the Co particles, achieving an electron-rich Co surface. The presence of Zn promoted the dissociation of H$_2$ and lowered the diffusion barrier of H atoms, speeding up the hydrogenation/hydrodeoxygenation processes. Furthermore, the doping of Zn lowered the barrier of breaking the C–OH bond of FFA and facilitated the subsequent hydrodeoxygenation

process of FFA, rendering it easily accessible to 2-MTHF. W. Golub *et al.* prepared an array of carbon-supported Co–Cu catalysts by using the mixed-metal MOF-74 as the precursor (Fig. 6c).[77] The Co–Cu MOF-derived bimetallic catalysts were featured with a Co-rich core and Cu-rich shell structure at a higher pyrolysis temperature, which led to high selectivity toward FFA. At lower pyrolysis temperatures (<600 °C), the catalyst featured more exposed Co in the Cu shell, exhibiting high catalytic activity and 2-MF selectivity. Besides, the selectivity of the products could be modulated by altering the Co/Cu ratio, with higher 2-MF selectivity at higher Co/Cu ratios. Apart from the aforementioned Co-based metal-based catalysts, metal/metal oxides have also been used for the conversion from FFR to 2-MF. Koley *et al.* fabricated a Cu/CuFe$_2$O$_4$@C-A catalyst by employing the Fe-MIL-88B as the sacrificial template, giving 100% yield of 2-MF at 165 °C for 5 h (Fig. 6d).[78] Kinetic studies have shown that the Cu/CuFe$_2$O$_4$@C-A catalyst with dual active sites possesses a lower activation energy barrier, which facilitates the activation of a continuous hydrodeoxygenation process.

5. Catalytic hydrogenation of furfural to cyclopentanone or cyclopentanol.

Among the FFR-derived chemicals, cyclopentanone (CPO) holds great prospects due to its universal application in manufacturing biofuels, resins, perfumes and pesticides.[79] As widely reported, the hydrogenation and rearrangement of FFR to cyclic compounds must proceed through a sequence of steps including C=O hydrogenation, ring rearrangement, hydrogenation, and dehydration. The hydrogenation of FFR to CPO is catalyzed by metal-acid bifunctional catalysts, in which the Lewis acid sites are a critical factor in facilitating the rearrangement of the furan ring. The dissociated H$^+$ from water is essential to facilitate the rearrangement process from FFA to CPO. Therefore, the introduction of water is crucial in the hydrogenation of FFR to CP.

Most of the reported catalysts for the conversion of FFR to CPO are noble metal/MOF composites (Table 4). Fang *et al.* synthesized supported Ru particles on an acidic MOF material (Ru/MIL-101), which was used for the hydrogenation of FFR to CPO.[80] MIL-101 was selected as the support due to the large surface area, broad pore size, and excellent thermal stability, obtaining Ru particles with high dispersibility. The 3% Ru/MIL-101 catalyst gave 99% FFR conversion and 96% CPO selectivity within 2.5 h at 160 °C and 4 MPa H$_2$. Li *et al.* prepared a series of MIL-MOFs with Lewis acid sites for supporting noble metal particles (Pd, Ru, Pt, and Au) (Fig. 7a).[81] Noble metal/Fe-MIL-100 exhibited higher hydrogenation activity than Fe-MIL-101 and

Table 4   The conversion of FFR to CPO or CPA over MOF based catalysts

| MOF	Catalyst	Solvent	H_2 (MPa)	Temp. (°C)	Time (h)	FFR Conv. (%)	CPO Yield (%)	CPA yield	Ref.
MIL-101(Cr)	3% Ru/MIL-101	H_2O	4	160	2.5	99	96	–	80
Fe-MIL-100	Pd/Fe-MIL-100	H_2O	4	150	6	99	92.2	–	81
Fe-MIL-100	Au/Fe-MIL-100	H_2O	4	150	6	97.8	35.4	–	81
Fe-MIL-100	Pt/Fe-MIL-100	H_2O	4	150	6	98.1	19.7	–	81
UiO-66	Pd–Co@UiO-66	H_2O	3	120	12	99	95	–	82
UiO-66-NO_2	Pd/UiO-66-NO_2	H_2O	1	150	5	98.9	95.5	–	83
Cu-BTC	Pd/Cu-BTC	H_2O	4	150	6	96.4	93	–	84
NiCo-MOF	2Co-1Ni@NC-800	H_2O	1.5	150	6	100	92.5	–	49
Cu-BTC	$CuNi_{0.5}$@C	H_2O	5	130	5	99.3	96.9	–	85
ZIF-8@ZIF-67	H-3DOM-Co/NC-600	H_2O	2	180	8	100	–	97.8	87
ZIF-8/ZIF-67	4LH-Co@NC	H_2O	2	160	8	100	–	97	90
Ni-MOF	Ni/C-$Mo_{0.4}$	H_2O	2	140	2	100	–	95	91
NiCo-BTC	Ni1Co1@C	H_2O	1	160	1	100	–	96	70
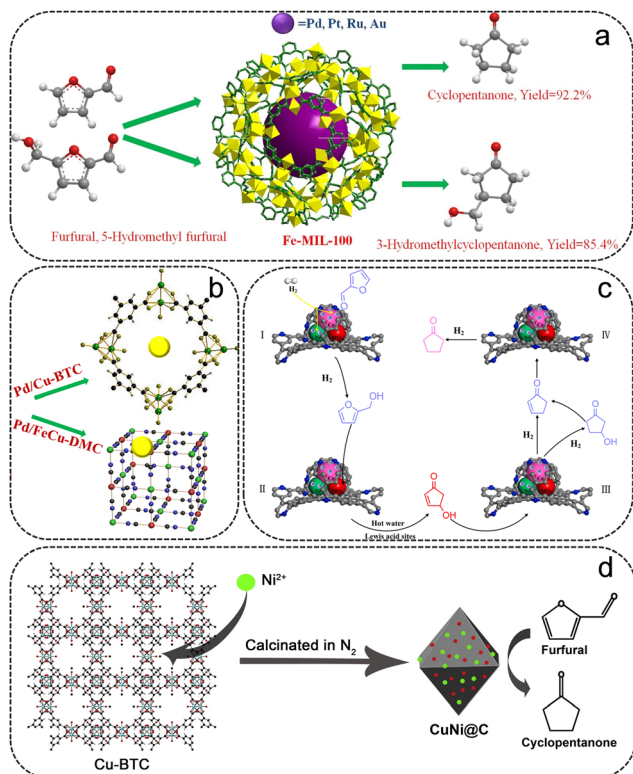
Fig. 7   (a) Schematic illustration of the conversion of FFR to CPO over noble metal/Fe-MIL-100 catalysts. Reproduced from ref. 81 with permission from Elsevier, copyright 2019. (b) Structure diagram of the Pd/Cu-BTC. Reproduced from ref. 84 with permission from Elsevier, copyright 2019. (c) Catalysis mechanism of FFR hydrogenation rearrangement to CPO. Reproduced from ref. 49 with permission from Elsevier, copyright 2021. (d) Schematic illustration of the synthesis of CuNi@C for FFR hydrogenation. Reproduced from ref. 85 with permission from Elsevier, copyright 2016.

Cr-MIL-101-based catalysts due to the availability of more active sites with highly dispersed particles. The high lipophilicity of the Fe ions in MOFs promoted the adsorption and hydrolysis of FFA, giving a high CPO selectivity for noble metals on Fe-MIL-101 and Fe-MIL-100. The Pd/Fe-MIL-100 catalyst exhibited the best catalytic activity, with 99% FFR conversion and 92.2% selectivity of CPO at 150 °C and 4 MPa H_2.

The excellent thermal and chemical stability of UiO-66 makes it an outstanding support for the loaded noble metal particles. Wang et al. designed a Pd–Co@UiO-66 catalyst with Pd–Co particles encapsulated in the framework of UiO-66 for the conversion of FFR to CPO.[82] The Pd–Co@UiO-66 showed higher catalytic performance with a 95% yield of CPO at 120 °C for 12 h than monometallic Pd@UiO-66, indicating a synergetic catalytic effect of trace Co with Pd metals. To increase the number of Lewis acid sites, –NO_2 modified UiO-66 was adopted as the support. Wang and their co-workers prepared highly dispersed Pd particles encapsulated in UiO-66-NO_2 (Pd/UiO-66-NO_2) by a double-solvent method followed by H_2 reduction.[83] After the heat treatment, more Lewis sites can be exposed owing to the creation of missing-linker defects. Therefore, the obtained defective Pd/UiO-66-NO_2 exhibited an excellent catalytic performance with 98.9% FFR conversion and 95.5% CPO selectivity at 150 °C for 5 h. An array of Pd particles loaded on Cu-MOFs with pure Lewis acidity were prepared for the hydrogenative ring-rearrangement reaction of FFR (Fig. 7b).[84] Due to the high surface area and homogeneous dispersion of the Pd particles as well as the strong acidity of Cu-BTC, Pd/Cu-BTC showed remarkable catalytic activity and stability.

Non-noble metals are increasingly being exploited for the conversion of FFR to CPO, including a few reported MOF-derived non-noble metal catalysts. Huang et al. fabricated a series of N-doped bimetallic catalysts (CoNi@NC) by employing NiCo-MOFs as the precursor.[49] Among them, 2Co-1Ni@NC-800 displayed the highest CPO yield (92.5%) at 150 °C and 1 MPa H_2 for 5 h. It was shown that there exist active Lewis acid sites in CoO_x and NiO on the surface of 2Co-1Ni@NC-800, which is favorable to the arrangement process of FFA. Additionally, the catalytic mechanism of FFR hydrogenation to CPO was proposed (Fig. 7c). First, the FFR and H_2 are absorbed at the active sites on the catalyst surface, where the FFR is converted to FFA. Then, the rearrangement reaction occurs at the Lewis active sites, followed by a hydrogenation reaction to convert the FFA to CPO. The excellent stability of the 2Co-1Ni@NC-800 catalyst is closely related to the tightly wrapped C–N layer coated around the metal particles, which restricts the loss of metal particles in the reaction process. The Cu-based catalyst was reported to be effective in activating the C=O bond, and

This journal is © The Royal Society of Chemistry and the Chinese Chemical Society 2023

the addition of Ni displayed a synergistic effect to be capable of enhancing the activity of FFR towards CPO. Wang *et al.* employed Cu-BTC as the precursor to impregnate Ni ions for fabricating CuNi bimetallic catalysts (Fig. 7d).[85] The MOF-derived porous carbon can not only act as a support but also prevent the metal particles from accumulating. Using CuNi$_{0.5}$@C as the catalyst, 99.3% FFR conversion and 96.9% CPO yield were obtained within 5 h at 130 °C and 5 MPa H$_2$.

Cyclopentanol (CPA) is the simplest member of the cyclopentanol's group with a single hydroxyl substituent, which is used in the production of perfumes, chemical solvents, dye intermediates, pharmaceuticals and other organic products.[86] CPA is the hydrogenation product of CPO, to the best of our knowledge, catalyzed by MOF-derived non-noble metal catalysts (Table 4). Although MOFs can serve as the ideal and versatile templates for fabricating metal/carbon materials, most of the composites obtained contain only microspores, limiting the mass transfer of the reaction substrates. Recently, ordered macroporous structures were obtained by pyrolysis of the complexes of ZIF and 3D-ordered polystyrene spheres (PS).[87–89] Yao *et al.* fabricated a 3D ordered macroporous Co/N-doped carbon composite with a hollow wall structure (H-3DOM-Co/NC) using an ordered ZIF-8@ZIF-67 as a precursor (Fig. 8a).[87] After the pyrolysis, the interconnected microporous structures are mostly preserved, leaving the pore wall with Co particles embedded in the hollow walls after the solid-to-hollow transformation. The 3D-ordered macroporous structure facilitates the mass transfer and the hollow wall prompts the exposure of Co active sites, which enhances the catalytic performance of FFR to CPA. The unique hollow macroporous structure of the

H-3DOM-Co/NC-600 catalyst achieved a 97.8% yield of CPA in 8 h at 180 °C and 2 MPa H$_2$. Besides, the solid-to-hollow transformation process was also used to fabricate multi-shell hollow nanoarchitectures based on ZIF samples. Chen *et al.* proposed a strategy for the pyrolysis of multilayer solid ZIF-8/ZIF-67 prepared by a stepwise growth approach into a hollow Co@NC catalyst with a specific shell number (Fig. 8b).[90] The strategy has successfully synthesized multishell hollow structures. These unique multishell hollow structures tremendously facilitated the diffusion of the reactants and enhanced the exposure of the active Co sites, which contributed to the excellent catalytic performance for the selectivity hydrogenation of FFR to CPA. The as-prepared 4LH-Co@NC catalyst with a 4-shell structure exhibited the highest catalytic activity, giving complete FFR conversion and 97% selectivity of CPA at 180 °C and 2 MPa H$_2$ for 8 h. The basic sites stabilized the intermediates in the conversion process of FFA, and the acid sites activated the opening process of the furan ring and the cyclization rearrangement reaction, both of which guaranteed the high selectivity of CPA.

Mo-based catalysts have been reported to be highly effective in water-based hydrodeoxygenation processes, but few researchers have used Mo-based catalysts for rearrangement reactions. Xia *et al.* designed a NiMo bimetallic catalyst derived from a Mo-containing Ni-MOF, which is used for the selectivity rearrangement reactions of FFR to CPA.[91] The Ni/C-Mo$_{0.4}$ catalyst achieved the highest selectivity of CPA (95%) under mild conditions. Besides, other Ni-based bimetallic catalysts (Ni/C–Fe, Ni/C–Zn, Ni/C–Cu, and Ni/C–Ce) were also synthesized and exhibited lower catalytic activity. Therefore, the addition of the element Mo could synergistically react with Ni to facilitate the transformation of FFR to CPA. This group also prepared an efficient NiCo bimetallic catalyst with highly dispersed metal particles derived from NiCo-BTC.[70] The Ni1Co1@C catalyst gave complete FFR conversion and 96% selectivity of CPA in the aqueous medium. This demonstrated that the presence of water is a crucial factor in obtaining the desired product, enabling the arrangement of the furan ring.
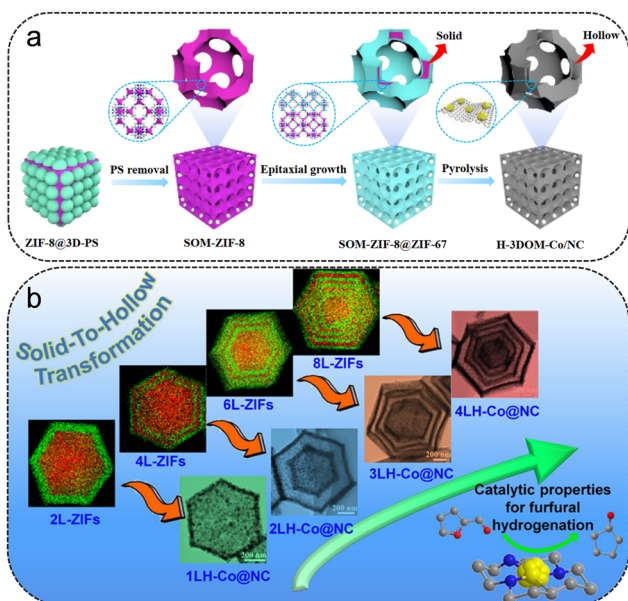
6. Catalytic hydrogenation of furfural to other high-value-added chemicals

Other value-added chemicals, such as 1,2-pentanediol (1,2-PD) and 1,5-pentanediol (1,5-PD), can also be obtained from the hydrogenation of FFR.[92,93] The hydrogenation of FFR to pentanediols is a tandem reaction involving an initial conversion of FFR to FFA, followed by ring-opening to yield the targets 1,2-PD and 1,5-PD.[94] According to our investigations, only one MOF-based noble metal catalyst was employed to catalyze FFR to 1,5-PD. Yeh *et al. in situ* synthesized a novel Al-supported Pt catalyst (Pt@Al$_2$O$_3$) by employing Pt-embedded MIL-53(Al)-NH$_2$ as the precursor for the conversion of FFR to 1,5-PD under aqueous media.[95] The Pt@Al$_2$O$_3$ with a Pt loading of 11.8% gave a 75.2% yield of 1,5-PD at 45 °C and 0.45 MPa H$_2$ for 8 h. The Pt particles are highly distributed in the MOF-derived Al$_2$O$_3$

Fig. 8 (a) Schematic illustration of the synthesis process of H-3DOM-Co/NC. Reproduced from ref. 87 with permission from Wiley-VCH, copyright 2021. (b) Schematic illustration of the solid-to-hollow transformation of ZnCo-ZIF for FFR hydrogenation. Reproduced from ref. 90 with permission from American Chemical Society, copyright 2019.

supports owing to the strong interaction between the penta-hedrally coordinated Al^{3+} and Pt. The presence of Brønsted acid sites in Al_2O_3 facilitates the $NaBH_4$ hydrolysis and promotes reactivity. $NaBO_2$, the hydrolysis product of $NaBH_4$, was demonstrated to be a key factor to convert FFR to 1,5-PD under mild conditions. In addition, Pt@Al_2O_3 has excellent stability and adaptability to various biomass-derived furan chemicals under $NaBH_4$-assisted hydrogenolysis. In brief, there are extremely few studies on the one-step conversion of MOF-based catalysts from FFR to 1,2-PD/1,5-PD with undesirable yields.

7. Conclusions and perspectives

This review tackles the challenge to give a full-scale overview of the most recent developments for the hydrogenation of FFR to high-value-added chemicals over MOF-derived catalysts. So far, the employment of heterogeneous MOF-based catalysts gave outstanding yields toward target molecules and diversify the variety of the catalysts. MOF-based catalysts can be further classified into three types: MOFs or modified MOFs, MOF-based noble catalysts, and MOF-based non-noble catalysts, which can be summarized as follows:

(1) MOFs or modified MOFs: The intrinsic properties of MOFs, such as abundant Lewis active sites that exist in Zr-based MOFs (MOF-808, UiO-66, *etc.*), or basic/acid sites after modifying with $-NH_2$ or $-SO_3$, aid in exhibiting catalytic activity toward target reaction routes. Given the relatively mild hydrogenation conditions of FFR, MOFs/modified MOFs with abundant isolated catalytic active sites, large surface area and adjustable pore size can efficiently catalyze the hydrogenation reaction.

(2) MOF-based noble metal catalysts: These mainly encompass two types. One is the MOF framework as porous support with tunable pores acting as a cavity to anchor the noble metals, which is commonly used to prepare noble metal/MOF composites. The porous MOF shell nanostructures can prevent the aggregation of noble metal particles during the reaction, permit the mass transfer of reactants/products, and guarantee the accessibility of the metal active sites. The other is the synthesis of metals/MOF compounds first, followed by transformation to noble metals supported on a metal oxide catalyst with a large surface area and high thermal stability (mainly MIL-101, UiO-66, and MIL-100). This *in situ* strategy demonstrates great flexibility in immobilizing various mono- and bimetallic metals in different MOFs compared to the above-mentioned metal/MOF composites.

(3) MOF-based non-noble metal catalysts: This mainly contains two preparation methods. One is a one-step synthesis of non-noble metal mono- or bimetallic catalysts using Ni, Co, and Cu-based MOFs (Ni-BTC, NiCu-BTC, ZIF-67, CuCo-ZIF, CoCu-MOF-74, *etc.*) as sacrificing templates, in which the porous carbon derived from organic ligands can prevent the metal particles from aggregation. Another is the introduction of active metal ions into the MOF precursor first (Ni-BTC, Cu-BTC, and ZIF-67), followed by *in situ* conversion to bimetallic catalysts or metal/metal oxide composites embedded in porous carbon. The synergistic interaction between the metals can efficiently catalyze the conversion of FFR to specific target products.

The development of highly efficient catalysts remains a research emphasis for the conversion of FFR to high value-added chemicals. Given the highly reactive properties of both the furan ring and the aldehyde group contained in the FFR molecule, selective hydrogenation of FFR to target products is a challenge. Many attempts have been devoted and considerable progress has been achieved in noble metal catalysts (Pt, Ru, and Pd-based) and non-noble metal catalysts (Cu, Ni, and Co-based). The four main routes of FFR hydrogenation reactions in this review are highlighted as follows:

The conversion of FFR to FFA involves the hydrogenation of the carbonyl group while inhibiting the hydrogenation of the furan ring, which poses a great challenge for the designing and preparing of the catalyst. Currently, MOF-derived precious metal catalysts catalyze the conversion of FFR mainly under moderate conditions (0.2–1 MPa H_2, 20–80 °C), while non-precious metal catalysts demand relatively rigorous conditions (1–4 MPa H_2, 120–180 °C). Besides, the CTH reaction with short-chain alcohols substituting H_2 has been proven to be a promising alternative for the highly selective conversion of FFR to FFA. For obtaining THFA by FFR, the hydrogenation of both the carbonyl group and the furan ring is compulsory, which imposes high demands on the hydrogenation activity of the catalysts. Generally, MOF-derived Ni-based mono- and bimetallic catalysts were used for converting FFR to THFA and good performance was achieved. Pd-based metal catalysts derived from MOFs were the only noble metals employed for the preparation of THFA, uncovering the high activation ability of Pd metals on furan rings. The transformation of FFR to 2-MF or 2-MTHF involves initial FFR hydrogenation to obtain FFA or THFA, followed by the hydrogenolysis of the C–O bond, a more complicated reaction path and requiring demanding catalytic conditions. To date, there are only a limited number of MOF-derived non-precious metal catalysts (Co and Cu-based) available for this route. The unsatisfactory yields and harsh reaction conditions have prompted intensive investigations on the reaction mechanism for designing efficient catalysts and achieving outstanding achievements. Complicated steps including C=O hydrogenation, ring rearrangement, hydrogenation and dehydration are necessary for converting FFR to CPO to realize both the hydrogenation and rearrangement processes, thus requiring a metal–acid bifunctional catalyst. The presence of water is crucial as the dissociated H^+ from water plays an overwhelming role in facilitating the rearrangement process. Based on the reported literature, many endeavors have been made and satisfactory progress has been achieved for MOF-derived noble metal catalysts (Pd, Pt, Au, and Ru-based) as well as non-precious metal catalysts (Co, Ni, and Cu-based). Nevertheless, there remains a long way to go in expediting the industrial production of FFR to CPO or CPA.

Although considerable progress has been achieved in the hydrogenation of FFR to high-value-added chemicals over

MOF-based catalysts, the dilemmas of the insufficiency of insight into the reaction mechanism, the determination of the adsorption configuration of the reactants and the rigorous reaction conditions still remain. Therefore, further exploration is needed to uncover the reaction mechanism of each reaction pathway to better design catalysts to catalyze the conversion of FFR to target molecules. Besides, the adsorption configurations of the reactant/intermediate molecules on different metal surfaces should be better clarified so that appropriate catalysts can be chosen for different target products. Finally, it is worth underlining that MOF-derived catalysts should undergo rational modulation to achieve hydrogenation of FFR under mild conditions for early realization of the transition from the laboratory to industrial scale. In summary, there remains great potential in designing and modulating MOF-based catalysts for the upgrading of FFR molecules.

Conflicts of interest

There are no conflicts to declare.

Acknowledgements

Notes and references

1 X. Shen, C. Zhang, B. Han and F. Wang, Catalytic self-transfer hydrogenolysis of lignin with endogenous hydrogen: Road to the carbon-neutral future, *Chem. Soc. Rev.*, 2022, **51**, 1608–1628.

2 C. Mondelli, G. Gozaydin, N. Yan and J. Perez-Ramirez, Biomass valorisation over metal-based solid catalysts from nanoparticles to single atoms, *Chem. Soc. Rev.*, 2020, **49**, 3764–3782.

3 H. Zhang, H. Li, C. Xu and S. Yang, Heterogeneously chemo/enzyme-functionalized porous polymeric catalysts of high-performance for efficient biodiesel production, *ACS Catal.*, 2019, **9**, 10990–11029.

4 X. Li, P. Jia and T. Wang, Furfural: A promising platform compound for sustainable production of C_4 and C_5 chemicals, *ACS Catal.*, 2016, **6**, 7621–7640.

5 C. Xu, E. Paone, D. Rodriguez-Padron, R. Luque and F. Mauriello, Recent catalytic routes for the preparation and the upgrading of biomass derived furfural and 5-hydroxymethylfurfural, *Chem. Soc. Rev.*, 2020, **49**, 4273–4306.

6 K. Yan, G. Wu, T. Lafleur and C. Jarvis, Production, properties and catalytic hydrogenation of furfural to fuel additives and value-added chemicals, *Renewable Sustainable Energy Rev.*, 2014, **38**, 663–676.

7 M. Besson, P. Gallezot and C. Pinel, Conversion of biomass into chemicals over metal catalysts, *Chem. Rev.*, 2014, **114**, 1827–1870.

8 Y. Yang, Z. Ren, S. Zhou and M. Wei, Perspectives on multifunctional catalysts derived from layered double hydroxides toward upgrading reactions of biomass resources, *ACS Catal.*, 2021, **11**, 6440–6454.

9 Z. An and J. Li, Recent advances in the catalytic transfer hydrogenation of furfural to furfuryl alcohol over heterogeneous catalysts, *Green Chem.*, 2022, **24**, 1780–1808.

10 W. Fang and A. Riisager, Recent advances in heterogeneous catalytic transfer hydrogenation/hydrogenolysis for valorization of biomass-derived furanic compounds, *Green Chem.*, 2021, **23**, 670–688.

11 Y. Nakagawa, M. Tamura and K. Tomishige, Catalytic reduction of biomass-derived furanic compounds with hydrogen, *ACS Catal.*, 2013, **3**, 2655–2668.

12 Z. Zhao, R. Bababrik, W. Xue, Y. Li, N. M. Briggs, D.-T. Nguyen, U. Nguyen, S. P. Crossley, S. Wang, B. Wang and D. E. Resasco, Solvent-mediated charge separation drives alternative hydrogenation path of furanics in liquid water, *Nat. Catal.*, 2019, **2**, 431–439.

13 D. Wang, W. Gong, J. Zhang, M. Han, C. Chen, Y. Zhang, G. Wang, H. Zhang and H. Zhao, Encapsulated Ni-Co alloy nanoparticles as efficient catalyst for hydrodeoxygenation of biomass derivatives in water, *Chin. J. Catal.*, 2021, **42**, 2027–2037.

14 H. Wang, X. Li, X. Lan and T. Wang, Supported ultrafine NiCo bimetallic alloy nanoparticles derived from bimetal-organic frameworks: A highly active catalyst for furfuryl alcohol hydrogenation, *ACS Catal.*, 2018, **8**, 2121–2128.

15 Y. Zheng, R. Zhang, L. Zhang, Q. Gu and Z. A. Qiao, A resol-assisted cationic coordinative co-assembly approach to mesoporous ABO_3 perovskite oxides with rich oxygen vacancy for enhanced hydrogenation of furfural to furfuryl alcohol, *Angew. Chem., Int. Ed.*, 2021, **60**, 4774–4781.

16 K. Yang, Y. Li, R. Wang, Q. Li, B. Huang, X. Guo, Z. Zhu, T. Su and H. Lü, Synthesis of dual-active-sites Ni-Ni_2In catalysts for selective hydrogenation of furfural to furfuryl alcohol, *Fuel*, 2022, **325**, 124898.

17 L. Yan, Y. Xu, P. Chen, S. Zhang, H. Jiang, L. Yang, Y. Wang, L. Zhang, J. Shen, X. Zhao and L. Wang, A freestanding 3D heterostructure film stitched by MOF-derived carbon nanotube microsphere superstructure and reduced graphene oxide sheets: A superior multifunctional electrode for overall water splitting and Zn-Air batteries, *Adv. Mater.*, 2020, **32**, 2003313.

18 X. Zhao, B. Xiao, A. J. Fletcher, K. M. Thomas, D. Bradshaw and M. J. Rosseinsky, Hysteretic adsorption and desorption of hydrogen by nanoporous metal–organic frameworks, *Science*, 2004, **306**, 1012–1015.

19 L. Yang, L. Yan, Y. Wang, Z. Liu, J. He, Q. Fu, D. Liu, X. Gu, P. Dai, L. Li and X. Zhao, Adsorption site selective occupation strategy within a metal–organic framework for highly efficient sieving acetylene from carbon dioxide, *Angew. Chem., Int. Ed.*, 2021, **60**, 4570–4574.

20 Y. Liu, X. Liu, L. Feng, L. Shao, S. Li, J. Tang, H. Cheng, Z. Chen, R. Huang, H. Xu and J. Zhuang, Two-dimensional metal–organic framework nanosheets: Synthesis and applications in electrocatalysis and photocatalysis, *Chem-SusChem*, 2022, e202102603.

21 A. Bavykina, N. Kolobov, I. S. Khan, J. A. Bau, A. Ramirez and J. Gascon, Metal–organic frameworks in heterogeneous catalysis: Recent progress, new trends, and future perspectives, *Chem. Rev.*, 2020, **120**, 8468–8535.

22 D. Li, H. Xu, L. Jiao and H. Jiang, Metal–organic frameworks for catalysis: State of the art, challenges, and opportunities, *EnergyChem*, 2019, **1**, 100005.

23 N. Aljammal, C. Jabbour, J. W. Thybaut, K. Demeestere, F. Verpoort and P. M. Heynderickx, Metal–organic frameworks as catalysts for sugar conversion into platform chemicals: State-of-the-art and prospects, *Coord. Chem. Rev.*, 2019, **401**, 213064.

24 Z. Fang, B. Bueken, D. E. De Vos and R. A. Fischer, Defect-engineered metal–organic frameworks, *Angew. Chem., Int. Ed.*, 2015, **54**, 7234–7254.

25 X. Zhang, C. Yang, P. An, C. Cui, Y. Ma, H. Liu, H. Wang, X. Yan, G. Li and Z. Tang, Creating enzyme-mimicking nanopockets in metal–organic frameworks for catalysis, *Sci. Adv.*, 2022, **8**, eadd5678.

26 P. Li, K. Aranishi and Q. Xu, ZIF-8 immobilized nickel nanoparticles: Highly effective catalysts for hydrogen generation from hydrolysis of ammonia borane, *Chem. Commun.*, 2012, **48**, 3173–3175.

27 N. Tsumori, L. Chen, Q. Wang, Q. Zhu, M. Kitta and Q. Xu, Quasi-MOF: Exposing inorganic nodes to guest metal nanoparticles for drastically enhanced catalytic activity, *Chem*, 2018, **4**, 845–856.

28 H. Jiang, L. Yan, S. Zhang, Y. Zhao, X. Yang, Y. Wang, J. Shen, X. Zhao and L. Wang, Electrochemical surface restructuring of phosphorus-doped carbon@MoP electrocatalysts for hydrogen evolution, *Nano-Micro Lett.*, 2021, **13**, 215.

29 S. Zhang, P. Dai, H. Liu, L. Yan, H. Song, D. Liu and X. Zhao, Metal–organic framework derived porous flakes of cobalt chalcogenides (CoX, X = O, S, Se and Te) rooted in carbon fibers as flexible electrode materials for pseudocapacitive energy storage, *Electrochim. Acta*, 2021, **369**, 137681.

30 H. Ye, L. Li, D. Liu, Q. Fu, F. Zhang, P. Dai, X. Gu and X. Zhao, Sustained-release method for the directed synthesis of ZIF-derived ultrafine Co-N-C ORR catalysts with embedded Co quantum dots, *ACS Appl. Mater. Interfaces*, 2020, **12**, 57847–57858.

31 J. Guo, Y. Qin, Y. Zhu, X. Zhang, C. Long, M. Zhao and Z. Tang, Metal–organic frameworks as catalytic selectivity regulators for organic transformations, *Chem. Soc. Rev.*, 2021, **50**, 5366–5396.

32 R. Mariscal, P. Maireles-Torres, M. Ojeda, I. Sádaba and M. López Granados, Furfural: A renewable and versatile platform molecule for the synthesis of chemicals and fuels, *Environ. Sci.*, 2016, **9**, 1144–1189.

33 R. Fang, A. Dhakshinamoorthy, Y. Li and H. Garcia, Metal organic frameworks for biomass conversion, *Chem. Soc. Rev.*, 2020, **49**, 3638–3687.

34 M. Zhao, N. Yang, Z. Li and H. Xie, MOFs derived catalysts prepared by pyrolysis for hydrogenation of bio-based furfural: A mini-review, *ChemistrySelect*, 2020, **5**, 13681–13689.

35 A. Halilu, T. H. Ali, A. Y. Atta, P. Sudarsanam, S. K. Bhargava and S. B. Abd, Hamid, Highly selective hydrogenation of biomass-derived furfural into furfuryl alcohol using a novel magnetic nanoparticles catalyst, *Energy Fuels*, 2016, **30**, 2216–2226.

36 A. Aijaz, T. Akita, N. Tsumori and Q. Xu, Metal–organic framework-immobilized polyhedral metal nanocrystals: Reduction at solid–gas interface, metal segregation, core-shell structure, and high catalytic activity, *J. Am. Chem. Soc.*, 2013, **135**, 16356–16359.

37 T. W. Goh, C. K. Tsung and W. Huang, Spectroscopy identification of the bimetallic surface of metal–organic framework-confined Pt-Sn nanoclusters with enhanced chemoselectivity in furfural hydrogenation, *ACS Appl. Mater. Interfaces*, 2019, **11**, 23254–23260.

38 S. Sohrabi, R. K. Abasabadi, A. A. Khodadadi, Y. Mortazavi and A. Hoseinzadeh, *In situ* one-step deposition of highly dispersed palladium nanoparticles into zirconium metal–organic framework for selective hydrogenation of furfural, *Mol. Catal.*, 2021, **514**, 111859.

39 Q. Yuan, D. Zhang, L. Van Haandel, F. Ye, T. Xue, E. Hensen and Y. Guan, Selective liquid phase hydrogenation of furfural to furfuryl alcohol by Ru/Zr-MOFs, *J. Mol. Catal. A: Chem.*, 2015, **406**, 58–64.

40 R. Fang, L. Chen, Z. Shen and Y. Li, Efficient hydrogenation of furfural to fufuryl alcohol over hierarchical MOF immobilized metal catalysts, *Catal. Today*, 2021, **368**, 217–223.

41 Y. Long, S. Song, J. Li, L. Wu, Q. Wang, Y. Liu, R. Jin and H. Zhang, Pt/CeO$_2$@MOF core@shell nanoreactor for selective hydrogenation of furfural via the channel screening effect, *ACS Catal.*, 2018, 8506–8512.

42 B. Zhang, Y. Pei, R. V. Maligal-Ganesh, X. Li, A. Cruz, R. J. Spurling, M. Chen, J. Yu, X. Wu and W. Huang, Influence of Sn on stability and selectivity of Pt-Sn@UiO-66-NH$_2$ in furfural hydrogenation, *Ind. Eng. Chem. Res.*, 2020, **59**, 17495–17501.

43 W. W. Lestari, R. S. R. Suharbiansah, L. Larasati, F. Rahmawati, U. S. F. Arrozi, S. Durini, F. Rohman, R. Iskandar and E. Hey-Hawkins, A zirconium(IV)-based metal–organic framework modified with ruthenium and palladium nanoparticles: Synthesis and catalytic performance for selective hydrogenation of furfural to furfuryl alcohol, *Chem. Pap.*, 2022, **76**, 4719–4731.

44 M. Zahid, J. Li, A. Ismail, F. Zaera and Y. Zhu, Platinum and cobalt intermetallic nanoparticles confined within MIL-101(Cr) for enhanced selective hydrogenation of the carbonyl bond in α,β-unsaturated aldehydes: Synergistic effects of electronically modified Pt sites and Lewis acid sites, *Catal. Sci. Technol.*, 2021, **11**, 2433–2445.

45 Z. Li, Y. Shen, Q. Zhang and T. Hu, Budget MOF-derived catalyst to realize full conversion from furfural to furfuryl alcohol, *Mol. Catal.*, 2022, **518**, 112092.

640 | *Mater. Chem. Front.*, 2023, **7**, 628–642

This journal is © The Royal Society of Chemistry and the Chinese Chemical Society 2023

46 X. Yang, W. Liu, F. Tan, Z. Zhang, X. Chen, T. Liang and C. Wu, A robust strategy of homogeneously hybridizing silica and Cu₃(BTC)₂ to in situ synthesize highly dispersed copper catalyst for furfural hydrogenation, *Appl. Catal., A*, 2020, **596**, 117518.

47 K. Chen, J. Ling and C. Wu, *In situ* generation and stabilization of accessible Cu/Cu₂O heterojunctions inside organic frameworks for highly efficient catalysis, *Angew. Chem., Int. Ed.*, 2019, **58**, 2–9.

48 Y. Wang, Y. Miao, S. Li, L. Gao and G. Xiao, Metal–organic frameworks derived bimetallic Cu-Co catalyst for efficient and selective hydrogenation of biomass-derived furfural to furfuryl alcohol, *Mol. Catal.*, 2017, **436**, 128–137.

49 L. Huang, F. Hao, Y. Lv, Y. Liu, P. Liu, W. Xiong and H. Luo, MOF-derived well-structured bimetallic catalyst for highly selective conversion of furfural, *Fuel*, 2021, **289**, 119910.

50 F. Hu, Y. Wang, S. Xu, Z. Zhang, Y. Chen, J. Fan, H. Yuan, L. Gao and G. Xiao, Efficient and selective Ni/Al₂O₃-C catalyst derived from metal–organic frameworks for the hydrogenation of furfural to furfuryl alcohol, *Catal. Lett.*, 2019, **149**, 2158–2168.

51 W. Gong, Y. Lin, C. Chen, M. Al-Mamun, H. Lu, G. Wang, H. Zhang and H. Zhao, Nitrogen-doped carbon nanotube confined Co-Nₓ sites for selective hydrogenation of biomass-derived compounds, *Adv. Mater.*, 2019, e1808341.

52 J. G. Lee, S. Yoon, E. Yang, J. H. Lee, K. Song, H. R. Moon and K. An, Structural evolution of ZIF-67-derived catalysts for furfural hydrogenation, *J. Catal.*, 2020, **392**, 302–312.

53 Z. Li, Y. Shen, W. Cui, Q. Zhang and T. Hu, MOF derived non-noble metal catalysts to control the distribution of furfural selective hydrogenation products, *Mol. Catal.*, 2021, **513**, 111824.

54 Y. Fan, S. Li, Y. Wang, C. Zhuang, X. Liu, G. Zhu and X. Zou, Tuning the synthesis of polymetallic-doped ZIF derived materials for efficient hydrogenation of furfural to furfuryl alcohol, *Nanoscale*, 2020, **12**, 18296–18304.

55 S. Li, Y. Fan, C. Wu, C. Zhuang, Y. Wang, X. Li, J. Zhao and Z. Zheng, Selective hydrogenation of furfural over the Co-based catalyst: A subtle synergy with Ni and Zn dopants, *ACS Appl. Mater. Interfaces*, 2021, **13**, 8507–8517.

56 Y. Deng, R. Gao, L. Lin, T. Liu, X. Wen, S. Wang and D. Ma, Solvent tunes the selectivity of hydrogenation reaction over alpha-MoC catalyst, *J. Am. Chem. Soc.*, 2018, **140**, 14481–14489.

57 K. Wang, S. Liu, J. Zhang, Z. Hu, Q. Kong, Y. Xu and X. Huang, A one-stone-two-birds strategy to functionalized carbon nanocages, *ACS Nano*, 2022, **16**, 15008–15015.

58 A. H. Valekar, M. Lee, J. W. Yoon, J. Kwak, D. Hong, K. Oh, G. Cha, Y. Kwon, J. Jung, J. Chang and Y. K. Hwang, Catalytic transfer hydrogenation of furfural to furfuryl alcohol under mild conditions over Zr-MOFs: Exploring the role of metal node coordination and modification, *ACS Catal.*, 2020, **10**, 3720–3732.

59 Q. Fu, D. Liu, W. Niu, S. Zhang, R. Chen, Y. Wang, P. Zhao, H. Jiang, Y. Zhao, L. Yang, L. Yan, H. Wang and X. Zhao, Defect-engineered MOF-808 with highly exposed Zr sites as highly efficient catalysts for catalytic transfer hydrogenation of furfural, *Fuel*, 2022, **327**, 125085.

60 J. Wu, D. Liang, X. Song, T. Liu, T. Xu, S. Wang and Y. Zou, Sulfonic groups functionalized Zr-metal organic framework for highly catalytic transfer hydrogenation of furfural to furfuryl alcohol, *J. Energy Chem.*, 2022, **71**, 411–417.

61 M. Qiu, T. Guo, R. Xi, D. Li and X. Qi, Highly efficient catalytic transfer hydrogenation of biomass-derived furfural to furfuryl alcohol using UiO-66 without metal catalysts, *Appl. Catal., A*, 2020, **602**, 117719.

62 K. D. Agusta, M. F. Miharja, A. W. Sakti, U. S. F. Arrozi, L. Mukaromah, A. Patah, T. Hara and Y. Permana, Zr-MOFs-catalyzed transfer hydrogenation of furfural to furfuryl alcohol: Unveiled performance of DUT-52, *Mol. Catal.*, 2022, **524**, 112265.

63 M. S. Rahaman, S. Tulaphol, M. A. Hossain, M. C. Mulvehill, J. M. Spurgeon, T. Maihom and N. Sathitsuksanoh, Mechanism of transfer hydrogenation of carbonyl compounds by zirconium and hafnium-containing metal–organic frameworks, *Mol. Catal.*, 2022, **522**, 112247.

64 X. Meng, Y. Yang, L. Chen, M. Xu, X. Zhang and M. Wei, A control over hydrogenation selectivity of furfural via tuning exposed facet of Ni catalysts, *ACS Catal.*, 2019, **9**, 4226–4235.

65 P. Guo, S. Liao and X. Tong, Heterogeneous nickel catalysts derived from 2D metal–organic frameworks for regulating the selectivity of furfural hydrogenation, *ACS Omega*, 2019, **4**, 21724–21731.

66 Y. Su, C. Chen, X. Zhu, Y. Zhang, W. Gong, H. Zhang, H. Zhao and G. Wang, Carbon-embedded Ni nanocatalysts derived from MOFs by a sacrificial template method for efficient hydrogenation of furfural to tetrahydrofurfuryl alcohol, *Dalton Trans.*, 2017, **46**, 6358–6365.

67 Y. Su, Z. Li, H. Zhou, S. Kang, Y. Zhang, C. Yu and G. Wang, Ni/carbon aerogels derived from water induced self-assembly of Ni-MOF for adsorption and catalytic conversion of oily wastewater, *Chem. Eng. J.*, 2020, **402**, 126205.

68 Y. Wang, S. Liu, Q. Guo and Y. Zhang, Ni@C@CNT catalyst derived from CNT doped Ni-MOF for furfural hydrogenation to tetrahydrofurfuryl alcohol, *Asia-Pac. J. Chem. Eng.*, 2022, **17**, e2739.

69 F. Tang, L. Wang, M. Dessie Walle, A. Mustapha and Y. Liu, An alloy chemistry strategy to tailoring the d-band center of Ni by Cu for efficient and selective catalytic hydrogenation of furfural, *J. Catal.*, 2020, **383**, 172–180.

70 H. Xia, C. Chen, P. Liu, M. Zhou and J. Jiang, Selective hydrogenation of furfural for high-value chemicals: Effect of catalysts and temperature, *Sustainable Energy Fuels*, 2020, **4**, 5709–5720.

71 Y. Yang, D. Deng, D. Sui, Y. Xie, D. Li and Y. Duan, Facile preparation of Pd/UiO-66-v for the conversion of furfuryl alcohol to tetrahydrofurfuryl alcohol under mild conditions in water, *Nanomaterials*, 2019, **9**, 1698.

72 C. Wang, A. Wang, Z. Yu, Y. Wang, Z. Sun, V. M. Kogan and Y. Liu, Aqueous phase hydrogenation of furfural to tetrahydrofurfuryl alcohol over Pd/UiO-66, *Catal. Commun.*, 2021, **148**, 106178.

73 D. Yin, H. Ren, C. Li, J. Liu and C. Liang, Highly selective hydrogenation of furfural to tetrahydrofurfuryl alcohol over MIL-101(Cr)-NH₂ supported Pd catalyst at low temperature, *Chin. J. Catal.*, 2018, **39**, 319–326.

74 S. Pendem, S. R. Bolla, D. J. Morgan, D. B. Shinde, Z. Lai, L. Nakka and J. Mondal, Metal–organic-framework derived Co–Pd bond is preferred over Fe–Pd for reductive upgrading of furfural to tetrahydrofurfuryl alcohol, *Dalton Trans.*, 2019, **48**, 8791–8802.

75 P. Zhou, Y. Chen, P. Luan, X. Zhang, Z. Yuan, S. Guo, Q. Gu, B. Johannessen, M. Mollah, A. L. Chaffee, D. R. Turner and J. Zhang, Selective electrochemical hydrogenation of furfural to 2-methylfuran over a single atom Cu catalyst under mild pH conditions dagger, *Green Chem.*, 2021, **23**, 3028–3038.

76 L. Huang, L. Wang, Z. Zhang, X. Guo, X. Zhang, J. M. Chabu, P. Liu and F. Tang, Understanding the promotional effects of trace doped Zn in Co/NC for efficient one-pot catalytic conversion of furfural to 2-methyl-tetrahydrofuran, *J. Energy Chem.*, 2022, **71**, 225–233.

77 K. W. Golub, T. P. Sulmonetti, L. A. Darunte, M. S. Shealy and C. W. Jones, Metal–organic-framework-derived Co/Cu-carbon nanoparticle catalysts for furfural hydrogenation, *ACS Appl. Nano Mater.*, 2019, **2**, 6040–6056.

78 P. Koley, S. C. Shit, B. Joseph, S. Pollastri, Y. M. Sabri, E. L. H. Mayes, L. Nakka, J. Tardio and J. Mondal, Leveraging Cu/CuFe₂O₄-catalyzed biomass-derived furfural hydrodeoxygenation: A nanoscale metal–organic-framework template is the prime key, *ACS Appl. Mater. Interfaces*, 2020, **12**, 21682–21700.

79 X. Li, Z. Tong, S. Zhu, Q. Deng, S. Chen, J. Wang, Z. Zeng, Y. Zhang, J. Zou and S. Deng, Water-mediated hydrogen spillover accelerates hydrogenative ring-rearrangement of furfurals to cyclic compounds, *J. Catal.*, 2022, **405**, 363–372.

80 R. Fang, H. Liu, R. Luque and Y. Li, Efficient and selective hydrogenation of biomass-derived furfural to cyclopentanone using Ru catalysts, *Green Chem.*, 2015, **17**, 4183–4188.

81 X. Li, Q. Deng, L. Zhang, J. Wang, R. Wang, Z. Zeng and S. Deng, Highly efficient hydrogenative ring-rearrangement of furanic aldehydes to cyclopentanone compounds catalyzed by noble metals/MIL-MOFs, *Appl. Catal., A*, 2019, **575**, 152–158.

82 Y. Wang, C. Liu and X. Zhang, One-step encapsulation of bimetallic Pd-Co nanoparticles within UiO-66 for selective conversion of furfural to cyclopentanone, *Catal. Lett.*, 2020, **150**, 2158–2166.

83 C. Wang, Z. Yu, Y. Yang, Z. Sun, Y. Wang, C. Shi, Y. Liu, A. Wang, K. Leus and P. Van Der Voort, Hydrogenative ring-rearrangement of furfural to cyclopentanone over Pd/UiO-66-NO₂ with tunable missing-linker defects, *Molecules*, 2021, **26**, 5736.

84 Q. Deng, X. Wen and P. Zhang, Pd/Cu-MOF as a highly efficient catalyst for synthesis of cyclopentanone compounds from biomass-derived furanic aldehydes, *Catal. Commun.*, 2019, **126**, 5–9.

85 Y. Wang, S. Sang, W. Zhu, L. Gao and G. Xiao, CuNi@C catalysts with high activity derived from metal–organic frameworks precursor for conversion of furfural to cyclopentanone, *Chem. Eng. J.*, 2016, **299**, 104–111.

86 D. Li, Z. Tian, X. Cai, Z. Li, C. Zhang, W. Zhang, Y. Song, H. Wang and C. Li, Nature of polymeric condensates during furfural rearrangement to cyclopentanone and cyclopentanol over Cu-based catalysts, *New J. Chem.*, 2021, **45**, 22767–22777.

87 W. Yao, J. Chen, Y. Wang, R. Fang, Z. Qin, X. Yang and L. Chen, Nitrogen-doped carbon composites with ordered macropores and hollow walls, *Angew. Chem., Int. Ed.*, 2021, **60**, 23729–23734.

88 K. Shen, L. Zhang, X. Chen, L. Liu, D. Zhang, Y. Han, J. Chen, J. Long, R. Luque, Y. Li and B. Chen, Ordered macro-microporous metal–organic framework single crystals, *Science*, 2018, **359**, 206–210.

89 Y. Wang, G. Fan, S. Wang, Y. Li, Y. Guo, D. Luan, X. Gu and X. Lou, Implanting CoOₓ clusters on ordered macroporous ZnO nanoreactors for efficient CO₂ photoreduction, *Adv. Mater.*, 2022, e2204865.

90 H. Chen, K. Shen, Y. Tan and Y. Li, Multishell hollow metal/nitrogen/carbon dodecahedrons with precisely controlled architectures and synergistically enhanced catalytic properties, *ACS Nano*, 2019, **13**, 7800–7810.

91 H. Xia, J. Li, C. Chen, D. Wu, J. Ren, J. Jiang and M. Zhou, Selective aqueous-phase hydrogenation of furfural to cyclopentanol over Ni-based catalysts prepared from Ni-MOF composite, *Inorg. Chem. Commun.*, 2021, **133**, 108894.

92 X. Fu, X. Ren, J. Shen, Y. Jiang, Y. Wang, Y. Orooji, W. Xu and J. Liang, Synergistic catalytic hydrogenation of furfural to 1,2-pentanediol and 1,5-pentanediol with LDO derived from CuMgAl hydrotalcite, *Mol. Catal.*, 2021, **499**, 111298.

93 Y. Shao, M. Guo, J. Wang, K. Sun, L. Zhang, S. Zhang, G. Hu, L. Xu, X. Yuan and X. Hu, Selective conversion of furfural into diols over Co-based catalysts: Importance of the coordination of hydrogenation sites and basic sites, *Ind. Eng. Chem. Res.*, 2021, **60**, 10393–10406.

94 S. Liu, Y. Amada, M. Tamura, Y. Nakagawa and K. Tomishige, One-pot selective conversion of furfural into 1,5-pentanediol over a Pd-added Ir–ReOₓ/SiO₂ bifunctional catalyst, *Green Chem.*, 2014, **16**, 617–626.

95 J. Y. Yeh, B. M. Matsagar, S. Chen, H. L. Sung, D. C. W. Tsang, Y. Li and K. C. W. Wu, Synergistic effects of Pt-embedded, MIL-53-derived catalysts (Pt@Al₂O₃) and NaBH₄ for water-mediated hydrogenolysis of biomass-derived furfural to 1,5-pentanediol at near-ambient temperature, *J. Catal.*, 2020, **390**, 46–56.